

## Post Curing as an Effective Means of Ensuring the Long-term Reliability of PDMS Thin Films for Dielectric Elastomer Applications

Shamsul Zakaria, Frederikke Bahrt Madsen & Anne Ladegaard Skov

To cite this article: Shamsul Zakaria, Frederikke Bahrt Madsen & Anne Ladegaard Skov (2017) Post Curing as an Effective Means of Ensuring the Long-term Reliability of PDMS Thin Films for Dielectric Elastomer Applications, Polymer-Plastics Technology and Engineering, 56:1, 83-95, DOI: [10.1080/03602559.2016.1211689](https://doi.org/10.1080/03602559.2016.1211689)

To link to this article: <http://dx.doi.org/10.1080/03602559.2016.1211689>



View supplementary material [↗](#)



Accepted author version posted online: 16 Sep 2016.  
Published online: 16 Sep 2016.



Submit your article to this journal [↗](#)



Article views: 61



View related articles [↗](#)



View Crossmark data [↗](#)

## Post Curing as an Effective Means of Ensuring the Long-term Reliability of PDMS Thin Films for Dielectric Elastomer Applications

Shamsul Zakaria<sup>a,b</sup>, Frederikke Bahrt Madsen<sup>a</sup>, and Anne Ladegaard Skov<sup>a</sup>

<sup>a</sup>Danish Polymer Center, Department of Chemical and Biochemical Engineering, Technical University of Denmark, Kgs. Lyngby, Denmark;

<sup>b</sup>Faculty of Industrial Science and Technology, Universiti Malaysia Pahang, Gambang, Pahang, Malaysia

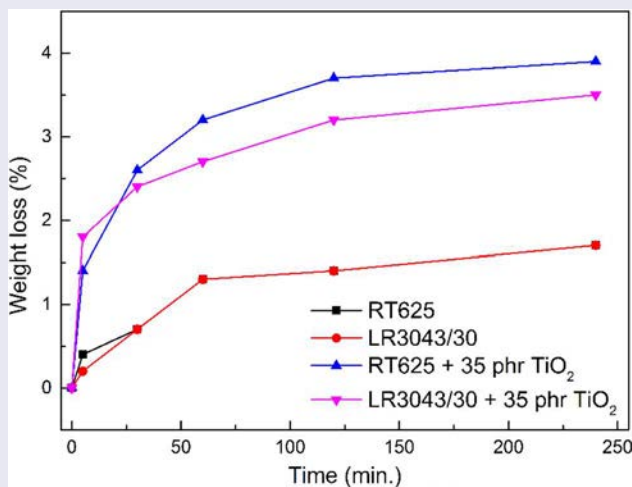
### ABSTRACT

Post curing can be used to facilitate volatile removal and thus produce polydimethylsiloxane (PDMS) films with stable elastic and electrical properties over time. In this study, the effect of post curing was investigated for commercial silicone elastomer thin films as a means of improving long-term elastomer film reliability. The Young's moduli and electrical breakdown strengths of commercial (silica-reinforced) PDMS elastomer films, with and without additional 35 parts per hundred rubber titanium dioxide (TiO<sub>2</sub>), were investigated after high-temperature (200°C) post curing for various time spans. The elastomers were found to contain less than 2% of volatiles (significantly higher for TiO<sub>2</sub>-filled samples), but nevertheless a strong effect from post curing was observed. The young's moduli as well as the strain-dependent behavior were found to change significantly upon post curing treatment, where Young's moduli at 5% strain increase with post curing. Furthermore, the determined dielectric breakdown parameters from Weibull analyses showed that greater electrical stability and reliability could be achieved by post curing the PDMS films before usage, and this method therefore paves a way toward more reliable dielectric elastomers.

### KEYWORDS

Ageing; elastomers; mechanical properties; silicones; thin films


### GRAPHICAL ABSTRACT



## Introduction

Silicone elastomers are used widely in various applications because of their many favorable properties, including their inherent softness, combined with low viscous dissipation as well as their temperature stability, which usually ranges from  $-100^{\circ}\text{C}$  to more than  $200^{\circ}\text{C}$ <sup>[1]</sup>. Due to their softness and elasticity, combined with their electrically insulating properties, silicone elastomers are one of the most used

materials for dielectric elastomers (DEs), which can be used in various products, such as lightweight and linear transducers, either in the form of generators (converting mechanical energy into electrical energy) or actuators (converting electrical energy into mechanical energy). This DE technology holds great promise due to the possibility of noiseless transduction, large strains, and low energy consumption, and so, silicone DE-based products

**CONTACT** Anne Ladegaard Skov ✉ [al@kt.dtu.dk](mailto:al@kt.dtu.dk)  Danish Polymer Center, Department of Chemical and Biochemical Engineering, Technical University of Denmark, Søtofts Plads, Building 227, 2800 Kgs. Lyngby, Denmark.

Color versions of one or more of the figures in this article is found online on at [www.tandfonline.com/lpte](http://www.tandfonline.com/lpte).

© 2017 Taylor & Francis

are currently being commercialized<sup>[2]</sup>. The optimization of the silicone elastomers—mainly with respect to obtaining increased dielectric permittivity and thus increased energy density—is manifested through various approaches, such as the covalent grafting of high permittivity moieties<sup>[3–6]</sup>, interpenetrating networks<sup>[7–11]</sup>, blending in high-permittivity oils<sup>[12,13]</sup>, and creating silicone elastomer composites with high-permittivity fillers such as metal oxides<sup>[14,15]</sup>. However, all modifications, to date, have resulted in one or more drawbacks. In general, not only is the dielectric breakdown strength of the DE reduced but also the overall lifetime of the silicone elastomer itself may be significantly altered. The lifetime and reliability of DEs are now more important than ever, especially with the emergence of the first commercial products. The reliability of the developed silicone DE transducers depends on the type of material used, fabrication techniques<sup>[16]</sup>, product design as well as transducer operating conditions, including the applied frequency, the amplitude of the applied voltage, and any prestraining of the elastomer. However, the reliability of optimized/modified silicone elastomers is often ignored, perhaps due to their reputation of being the most reliable material for DEs ever since the independent research center SRI International investigated various elastomer materials in the early 1990s<sup>[17]</sup>. They showed that the acrylic double-adhesive VHB 4910, produced by 3M, was the best-performing elastomer with respect to actuation strain at a given applied voltage and outperformed silicone-based elastomers over short time scales. Silicone elastomers, however, were shown to possess significantly faster actuation responses (in the order of milliseconds), greater reliability as well as negligible viscous loss compared to VHB<sup>[17]</sup>. However, an important and often ignored factor in filled silicone elastomers especially is the Mullins effect, i.e., the experienced maximum strain dependency of the elastic properties (stress softening). Precautions against these issues, however, can be taken<sup>[18]</sup>.

Silicone polymers are synthesized through the equilibrium polymerization of low molecular weight linear and cyclic siloxanes in the presence of acid or base catalysts. One disadvantage of this process is the formation of undesired by-products caused by a premature chain termination reaction and unreacted cyclic oligomers<sup>[19]</sup>. These residues are mobile within the resulting silicone elastomers, and under certain conditions, they outgas to the elastomer's surface or any device interface, thus leading to contamination (by the outgassing compounds). Siloxane oligomers from the polymerization process are a main contributor to silicone outgassing; nonetheless, they are compatible with the silicone elastomer matrix and may have very low vapor pressures, so the outgassing process is often very slow indeed<sup>[20]</sup>.

Furthermore, residual solvent from the manufacturing procedures may also exist in the cured film. The performance of many silicone elastomer-based devices is often altered by outgassing<sup>[21]</sup>, since outgassing changes the mechanical properties of elastomers, such as their tear strength and maximum elongation, due to the loss of a plasticizing effect from the oligomers<sup>[20]</sup>. Such uncontrolled changes in elastomer properties over time are naturally undesired. If the silicone elastomer is intended for use in human-contact products such as medical applications, post curing is mandatory to exclude outgassing in the final product. Post curing, however, is tedious and therefore generally avoided for other applications than medical. In post curing, the volatiles from the cross-linked silicone are normally removed by diffusion and evaporation at a higher temperature than the curing temperature. The rate at which this development proceeds depends on the physical and chemical properties of the utilized silicone as well as on the geometry and the design of devices (for example, the thickness and total surface area)<sup>[20]</sup>.

While several studies have investigated the effect outgassing of polymers<sup>[22]</sup>, rubbers<sup>[23]</sup>, resins<sup>[24,25]</sup>, and composites<sup>[26]</sup>, fewer studies have focused specifically on silicone elastomers<sup>[20,27]</sup> and to our knowledge, no studies exist on the effect of post curing on dielectric properties of silicone elastomers for dielectric elastomer applications. Rothka et al.<sup>[27]</sup> investigated the effect of post curing on the outgassing of silicone elastomers, which were initially post cured for 4 h at 204°C, resulting in a 2.7% mass loss. Subsequently, the post cured silicone elastomers were treated at 177°C for 20 h, and the observed mass loss was then less than 0.5%. In comparison, with no post curing, the mass loss at 177°C for 24 h was in the order of 4% (about eight times greater). It is thus evident that post curing is a key parameter in respect to outgassing.

Several methods to produce silicone elastomers with improved electromechanical properties have been developed<sup>[5,28–30]</sup>, with the addition of fillers, such as metal oxides<sup>[31–35]</sup>, being the most commonly investigated, due to the ease of elastomer formulation. Incorporating rigid fillers into silicone elastomers, though, changes intrinsic mechanical behavior such as the Mullins effect, as discussed earlier. In a previous study, we showed that nonpost cured elastomers with significant amounts of filler showed significant loss of tension over time upon prestraining to 120% for 3 months<sup>[36]</sup>.

Brook et al.<sup>[20]</sup> reported that post curing increases the Young's moduli of silicone elastomers. Since the dielectric breakdown strength of silicone elastomers is strongly dependent on the Young's modulus, dielectric breakdown strength is also very likely affected by post

curing<sup>[37]</sup>. Long-term mechanical and electrical reliability should be achievable if silicone elastomers are post cured before they are used in DE applications. Therefore, this study focuses on two types of silicone elastomers commonly utilized as DE materials, namely, commercial silicone elastomers, one with and one without an additional 35 phr permittivity-enhancing filler ( $\text{TiO}_2$ ), to investigate the effect of post curing on the mechanical and electrical stability of DEs. The study was performed by heating the cured silicone elastomers at 200°C for 0, 5, 30, 60, 120, and 240 min subsequent to the initial curing procedure. Most commonly used curing conditions for addition cure silicone elastomers are ~120°C for 10–30 min. The resulting mechanical and electrical properties of the various samples were then measured. To our knowledge, the effect of post curing on, for example, dielectric breakdown strength has not been investigated previously, since the fraction of volatiles is so low (usually stated to be 1–2% by the elastomer supplier) that it has—so far—seemed irrelevant.

## Experimental section

### Materials

Four different compositions of commercial silicone, with and without permittivity-enhancing filler, were investigated. The pristine elastomers were Elastosil RT625 A/B and Elastosil LR3040/30 A/B from Wacker Chemie AG. Elastosil RT625 A/B is a room-temperature vulcanising (RTV) elastomer, supplied as a two-part system. The utilized mixing ratio of parts A and B is 9:1. Elastosil LR3040/30 A/B is a high-viscosity liquid silicone rubber (LSR) which is also supplied as a two-part system. The utilized mixing ratio of parts A and B was 1:1, as recommended by the supplier. Both commercial elastomers are naturally filled with  $\text{SiO}_2$ . The choice of elastomers was based on previous experience with various types of commercial silicone elastomers, where the two chosen elastomers first of all provided acceptable viscosities for facile coating without the need for excessive amounts of solvent. Second, both elastomers provide good electrical breakdown strengths, and thus they are good candidates for dielectric elastomers.

The solvent OS-20 (an ozone-safe, volatile methylsiloxane fluid) was obtained from Dow Corning and was added to achieve a suitable viscosity for film coating. The OS-20 was added to the silicone formulation, as it also facilitates filler dispersion and thus produces more homogenous elastomer films. The choice of OS-20 solvent was based on feasibility in a large-scale production of DE thin films<sup>[38–40]</sup>.

The composites consist of the above-mentioned elastomers compounded with hydrophobic titanium

dioxide ( $\text{TiO}_2$ ) R420 from Sachtleben Chemie, with an average primary particle size of 250 nm. The particles were added in quantities of 35 parts per hundred rubber (phr), equating to a mass fraction of 26% in the final composite. The OS-20 was added to both silicone formulations with  $\text{TiO}_2$ . For clarity, the commercial silicone films will be referred to as pristine polydimethylsiloxane (PDMS) films, and composites containing additional 35 phr  $\text{TiO}_2$  will be referred to as filled PDMS elastomers.

### Sample preparation

Thin films were prepared based on the procedures described by Skov et al.<sup>[41]</sup> and as summarized below. Part B of the elastomer, some solvent and filler (in the case of the filled elastomer) were mixed by a DAC 150FVZ SpeedMixer (Hauschild Co.) at 3,000 rpm. After 5 min of mixing, part A of the material was added and mixed for another 5 min at 2,000 rpm. Glass plates were coated with the premixes, using a thin-film 3540 bird applicator from Elcometer. The films were cured in an oven for 5 min at 75°C and subsequently for 10 min at 115°C. The prepared films were removed from the glass plates before post curing was performed in a ventilated oven at 200°C for 0 (control), 5, 30, 60, 120, and 240 min. The thicknesses of the prepared films was around 52–105  $\mu\text{m}$ . Finally, the films were stored between 50- $\mu\text{m}$ -thick ethylene-tetrafluorethylene foils and kept in a desiccator until use.

### Methods

The volatile content measurements were performed on 150 × 50 mm PDMS films with thicknesses of 52–105  $\mu\text{m}$ . The weights of the PDMS films before and after 240 min of post curing were taken, and the weight loss percentages of the volatiles were then calculated. The differential scanning calorimetry (DSC) analysis was performed with a TA discovery DSC in an air atmosphere ranging from –90 to 100°C and at a heating rate of 10°C/min. The thermogravimetric analysis (TGA) was performed with a TA Discovery TGA. The films were heated in an air atmosphere up to 700°C and the heating rate was 10°C/min. Uniaxial extensional rheology was performed to determine the Young's modulus at different strains. Rectangular strips of approximately 6 mm × 20 mm and 52–105  $\mu\text{m}$  in thickness were prepared for the measurements, which were performed using an ARES-G2 with Sentmanat extensional rheology 2 (SER2) geometry. The SER2 has rotary clamps which are basically two cylinders winding up the sample, thus a stepwise increasing load

can be applied and the corresponding elongations can be measured. The test specimen was elongated uniaxially at a steady Hencky strain rate of 0.001 (/s). Young's moduli were obtained from the tangent of the stress-strain curves from 0 to 130% strains. Breakdown measurements were performed on an in-house built device based on international standards [IEC 60243-1 (1998) and IEC 60243-2 (2001)], and the film thicknesses (which can be found as supporting information) were determined with a Leica DMLB microscope replete with a USB Thorlabs 2.0 digital camera. The distance between the two spherical electrodes (with diameters of 20 mm) was set according to sample thickness with a micrometer stage and gauge. An indent of less than 3% of sample thickness was added to ensure that the spheres were in contact with the sample. A stepwise increasing voltage was applied (50–100 V/step) at a rate of 0.5–1.0 steps/s. Each sample was subjected to ten breakdown measurements, and an average of the values was stated as the breakdown strength of the sample. Furthermore, Weibull analysis was performed on the ten breakdown measurements to determine shape ( $\beta$ ) and scale ( $\eta$ ) parameters. Silver depositions were performed on a physical vapor deposition chamber system for reliable dielectric measurements, and this chamber was fitted with a large butterfly valve to control pumping speed and was pumped by an oil diffusion pump with a liquid nitrogen trap. The lid was lifted off the chamber whenever films or targets needed to be changed, and the lid wall seal was accomplished by the addition of a large ring. The base vacuum was approximately  $2 \times 10^{-5}$  bar. The chamber was fitted with an evaporation source (for silver), a DC magnetron sputter source, and an RF sputter source (for sputtering nonconducting targets). Silver evaporation was performed on the tungsten boat at the bottom of the chamber. According to the instrument calibration, this resulted in a sputtering rate of about 1.5 nm/s and produced a monolayer thickness of silver about 50–60 nm

within 30–40 s. Thin silver electrodes ensure sufficient contact between sample and plates. More details on the process can be found in Benslimane et al.<sup>[42]</sup> Dielectric relaxation spectroscopy was performed on a Novocontrol Alpha-A high-performance frequency analyser (Novocontrol Technologies GmbH & Co. KG, Germany) operating in the frequency range of  $10^{-1}$ – $10^6$  Hz at 23°C. Linear viscoelasticity for all samples was measured using an ARES-G2 rheometer (TA Instruments) set to a controlled strain mode, at 0.5% strain and with frequency sweeps from 100 to 0.01 Hz at ambient temperature, using a parallel-plate geometry of 25 mm in diameter. The elastomer samples for linear viscoelastic measurements were 25 mm in diameter and 0.5–1.3 mm thick. Frequency sweeps of the samples were measured at different post cure times (0, 5, 30, 60, 120, and 240 min). Time sweeps were performed on samples A (pure RT625), B (pure LR3040/30), C (RT625 + 35 phr TiO<sub>2</sub>), and D (LR3040/30 + 35 phr TiO<sub>2</sub>) at 0 and 240 min of post curing at a temperature of 200°C for 480 min at a constant strain of (0.5%) and frequency of (1 Hz). Temperature sweeps were likewise performed on these samples, using a temperature ramp mode within a temperature range of 20–200°C at a constant strain (0.5%) and frequency (1 Hz).

## Results and discussion

The content of volatiles in the samples was measured by examining the weight of the samples before and after the post curing treatment at 200°C for 5, 30, 60, 120, and 240 min. The results were calculated in terms of actual loss as a percentage as well as loss relative to the pure elastomer matrix for samples containing TiO<sub>2</sub>. The results are also shown in Table 1 and Figure 1.

From the results in Table 1 and Figure 1, it is clear that post curing filled elastomers results in a higher mass loss of volatiles compared to the two pristine silicone elastomers. During film preparation, solvent

**Table 1.** Weight loss of PDMS elastomer films after post curing for 5, 30, 60, 120, and 240 min. The weight loss of samples with TiO<sub>2</sub> is furthermore calculated relative to the commercial elastomer (by excluding the TiO<sub>2</sub> mass) for easy comparison with pure commercial elastomers.

| Sample ID | Material                            | 5 min    |  | 30 min   |  | 60 min   |  | 120 min  |  | 240 min  |  |
|-----------|-------------------------------------|----------|--|----------|--|----------|--|----------|--|----------|--|
|           |                                     | Loss (%) | Loss relative to elastomer matrix (excluding filler) (%) | Loss (%) | Loss relative to elastomer matrix (excluding filler) (%) | Loss (%) | Loss relative to elastomer matrix (excluding filler) (%) | Loss (%) | Loss relative to elastomer matrix (excluding filler) (%) | Loss (%) | Loss relative to elastomer matrix (excluding filler) (%) |
| A         | RT625                               | 0.4      | 0.4  | 0.7      | 0.7  | 1.0      | 1.0  | 1.1      | 1.1  | 1.2      | 1.2  |
| B         | LR3040/30                           | 0.2      | 0.2  | 0.7      | 0.7  | 1.3      | 1.3  | 1.4      | 1.4  | 1.7      | 1.7  |
| C         | RT625 + 35 phr TiO <sub>2</sub>     | 1.4      | 1.9  | 2.6      | 3.6  | 3.2      | 4.4  | 3.7      | 4.9  | 3.9      | 5.3  |
| D         | LR3040/30 + 35 phr TiO <sub>2</sub> | 1.8      | 2.4  | 2.4      | 3.2  | 2.7      | 3.7  | 3.2      | 4.3  | 3.5      | 4.7  |

phr, parts per hundred rubber.



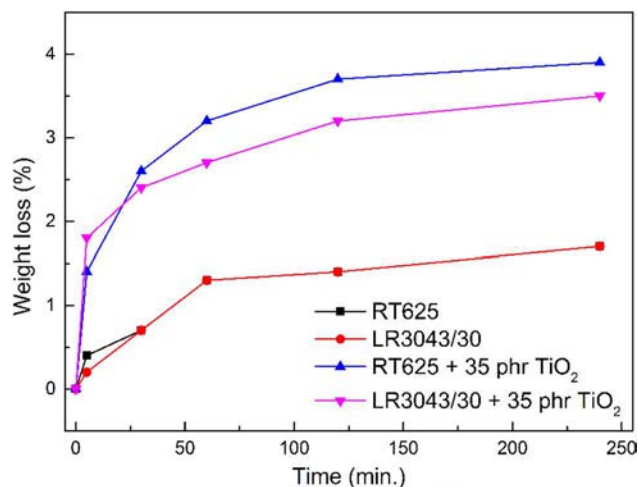


**Figure 1.** Weight loss as a function of post cure time.

and other volatiles may be adsorbed by the  $\text{TiO}_2$  particles, and thus these strongly influence the diffusion of volatiles during the initial cure. In principle, the solvent utilized for the filled samples should have been completely removed during curing, but from the results in Table 1, it is clear that the cured samples with  $\text{TiO}_2$  contain a higher fraction of volatiles. This again illustrates the importance of post curing especially for silicone elastomers with high filler content. It is also clear that outgassing depends not only on sample geometry but also, to a large extent, on sample composition. The two types of commercial elastomers may also consist of different types of silica and thus interactions in the resulting elastomer may be different from elastomer

type to the other. When the  $\text{TiO}_2$  particles are added, further deviations in behaviors may occur. It can also be seen from Figure 1 that most of the outgassing occurs within approximately 60 min, and thereafter only minor outgassing is taking place.

A determination of the content of volatiles in the films before and after post curing was undertaken using TGA. Figure 2 shows the TGA thermograms of the four elastomers after 0 and 240 min of post curing, respectively.

A time of 240 min was chosen as the maximum post curing time, as this is a commonly required treatment for thick silicone elastomers<sup>[20]</sup>. Samples without post curing show significant weight loss from room temperature to the first degradation process (around  $350^\circ\text{C}$ ) in the order of 3–5%. In comparison, samples which have been extensively post cured show significantly smaller weight loss over the same temperature range, as the volatiles inside the elastomer films have been effectively removed during the post curing process. The TGA thermograms for all samples post cured at the different time spans can be found as the supporting information.

The effect of post curing on thermal transition behavior in elastomers was examined by DSC. All thermograms for samples post cured at different time spans can be found as supporting information. An exothermic peak is observed for both the post cured and the non-post cured PDMS films during cooling, which corresponds to crystallization processes taking place in the films. During heating, an endothermic peak is observed, which corresponds to the crystallite melting. The

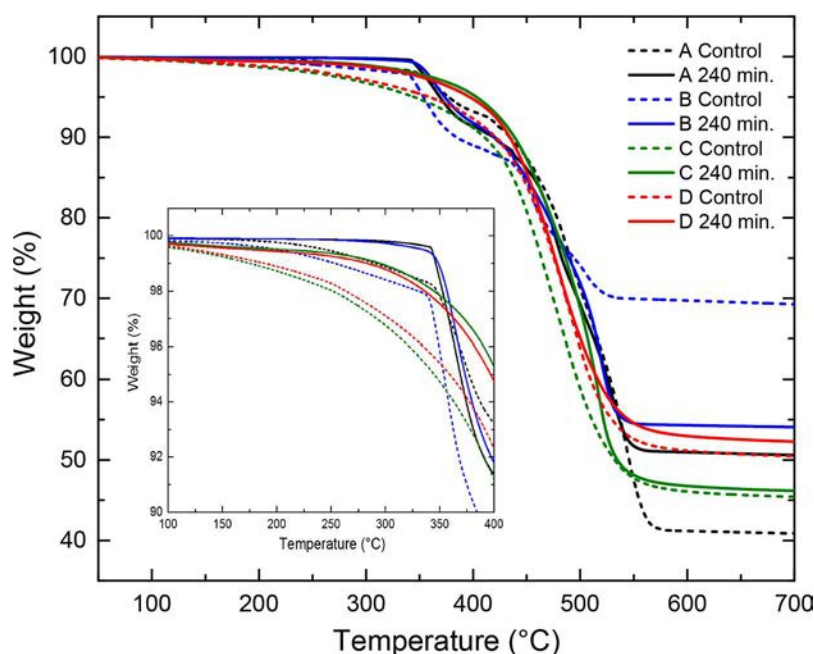


**Figure 2.** TGA thermograms for the investigated pristine and filled PDMS elastomer films with and without post curing treatment. Heating rate of  $10^\circ\text{C}/\text{min}$  in air atmosphere. (A = RT625, B = LR3040/30, C = RT625 + 35 phr  $\text{TiO}_2$ , D = LR3040/30 + 35 phr  $\text{TiO}_2$ ). Note: TGA, thermogravimetric analysis.

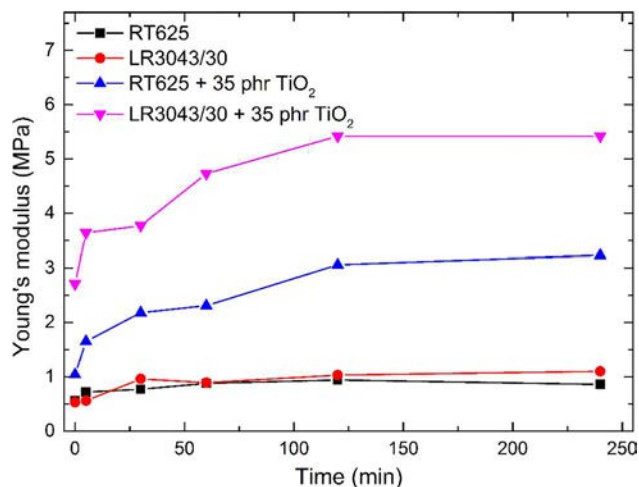


**Figure 3.** Young's modulus at 5% strain as a function of post cure time.

temperatures for which crystallization and melting occur are denoted by  $T_c$  and  $T_m$ , respectively. The DSC results indicate that post curing causes only a marginal effect on  $T_m$ . The results also indicate that the pristine PDMS films (A and B) exhibit lower  $T_c$  upon post curing. Inversely, upon post curing, the TiO<sub>2</sub>-filled PDMS films have higher than or similar  $T_c$  to their nonpost cured counterparts. The high filler content in the filled samples thus greatly influences the thermal behavior of the PDMS films. The glass transition temperatures,  $T_g$ , do not change significantly after post curing.

From the obtained results—so far—it is obvious that outgassing is to be expected if post curing is omitted during film fabrication. Thus, changes in the mechanical properties of the elastomer films over time are expected. To investigate these changes in mechanical properties with post curing time, the Young's modulus as a function of strain for the different samples was measured before and after post curing for different time spans. Figure 3 shows the Young's modulus at 5% strain as a function of post curing time.

The Young's moduli at 5% strain are furthermore summarized in Table 2 together with their percentage-wise increase induced by the post curing.

As seen in Figure 3 and Table 2, the Young's moduli of the control samples of the two pristine elastomers are in the same order of magnitude. After post curing, the Young's moduli, however, have increased to different extents. RT625 experienced a maximum increase of 68% following 120 min of post curing, while LR3040/30 experienced a maximum increase in the Young's modulus of 108% after 240 min of post curing. LR3040/30 thus becomes significantly stiffer than RT625 over time, probably due to the utilization of larger amounts of solvent during the processing. This also means that LR3040/30 will change more over time than RT625 if the post curing of samples is not performed prior to use as DEs. As seen in Figure 3 and Table 2, elastomers with TiO<sub>2</sub> experience a dramatic increase in the Young's modulus compared to the pristine

**Table 2.** Dielectric breakdown data and Young's moduli at 5% strain for different post cure times (A = RT625, B = LR3040/30, C = RT625 + 35 phr TiO<sub>2</sub>, D = LR3040/30 + 35 phr TiO<sub>2</sub>).

| Sample ID | Post cure time (min) | Breakdown strength (V/ $\mu$ m) | Increase in breakdown strength compared to control (%) | Thickness ( $\mu$ m) | Breakdown voltage (V) | Y at 5% strain (MPa) | Increase in Young's modulus compared to control (%) |
|-----------|----------------------|---------------------------------|--|----------------------|-----------------------|----------------------|---|
| A-Control | 0                    | 98 $\pm$ 4                      | —  | 69                   | 6,791                 | 0.56                 | —   |
| A-5 Min   | 5                    | 107 $\pm$ 3                     | 9.2  | 69                   | 7,419                 | 0.72                 | 28.6  |
| A-30 Min  | 30                   | 112 $\pm$ 5                     | 14.3   | 68                   | 7,683                 | 0.77                 | 37.5  |
| A-60 Min  | 60                   | 109 $\pm$ 4                     | 11.2   | 67                   | 7,368                 | 0.88                 | 57.1  |
| A-120 Min | 120                  | 115 $\pm$ 3                     | 17.3   | 67                   | 7,718                 | 0.94                 | 67.9  |
| A-240 Min | 240                  | 114 $\pm$ 4                     | 16.3   | 66                   | 7,545                 | 0.86                 | 53.6  |
| B-Control | 0                    | 108 $\pm$ 5                     | —  | 70                   | 7,566                 | 0.53                 | —   |
| B-5 Min   | 5                    | 106 $\pm$ 3                     | −1.9   | 69                   | 7,353                 | 0.56                 | 5.7   |
| B-30 Min  | 30                   | 117 $\pm$ 3                     | 8.3  | 68                   | 8,018                 | 0.96                 | 81.1  |
| B-60 Min  | 60                   | 119 $\pm$ 3                     | 10.2   | 68                   | 8,126                 | 0.89                 | 67.9  |
| B-120 Min | 120                  | 122 $\pm$ 3                     | 13.0   | 67                   | 8,195                 | 1.03                 | 94.3  |
| B-240 Min | 240                  | 126 $\pm$ 4                     | 16.7   | 67                   | 8,421                 | 1.10                 | 107.5   |
| C-Control | 0                    | 133 $\pm$ 6                     | —  | 53                   | 7,031                 | 1.04                 | —   |
| C-5 Min   | 5                    | 140 $\pm$ 4                     | 5.3  | 53                   | 7,460                 | 1.65                 | 58.7  |
| C-30 Min  | 30                   | 152 $\pm$ 5                     | 14.3   | 53                   | 8,083                 | 2.18                 | 109.6   |
| C-60 Min  | 60                   | 155 $\pm$ 5                     | 16.5   | 52                   | 8,098                 | 2.31                 | 121.2   |
| C-120 Min | 120                  | 165 $\pm$ 4                     | 24.1   | 52                   | 8,591                 | 3.06                 | 194.2   |
| C-240 Min | 240                  | 179 $\pm$ 6                     | 34.6   | 52                   | 9,305                 | 3.23                 | 210.6   |
| D-Control | 0                    | 138 $\pm$ 4                     | —  | 65                   | 8,911                 | 2.71                 | —   |
| D-5 Min   | 5                    | 141 $\pm$ 4                     | 2.2  | 65                   | 9,205                 | 3.64                 | 34.3  |
| D-30 Min  | 30                   | 147 $\pm$ 3                     | 6.5  | 65                   | 9,586                 | 3.77                 | 39.1  |
| D-60 Min  | 60                   | 158 $\pm$ 3                     | 14.5   | 63                   | 9,967                 | 4.73                 | 74.5  |
| D-120 Min | 120                  | 168 $\pm$ 3                     | 21.7   | 63                   | 10,593                | 5.42                 | 100   |
| D-240 Min | 240                  | 184 $\pm$ 3                     | 33.3   | 63                   | 11,790                | 5.42                 | 100   |

phr, parts per hundred rubber.

elastomers. This is expected when adding hard fillers to a silicone elastomer. Nevertheless, the samples do not experience similar increases despite having similar initial Young's moduli, possibly due to a difference in the composition of the two elastomers RT625 and LR3040/30. Upon post curing, the two elastomers with  $\text{TiO}_2$  also show different behaviors. The modulus of RT625 + 35 phr  $\text{TiO}_2$  increases by more than 200% after post curing, which thus has a dramatic effect upon the mechanical properties of the filled RT625. LR3040/30 + 35 phr  $\text{TiO}_2$  shows a modulus increase of 100%, which is comparable to what was experienced by its pristine counterpart. Furthermore, it applies to all samples that the Young's moduli are constant after 120 min of post curing. The pristine elastomers do, however, only need about 60 min to post cure. Young's modulus of all samples increases with post cure time, except a few cases (A 240 Min and B 60 Min) which is due to sample/measurement inaccuracies, since the trend is otherwise very clear for all samples.

Figure 4 illustrates stress–strain behavior up to 130% strain of elastomers before and after post curing for 240 min. The stress–strain curves clearly illustrate the stiffening effect of post curing, which is especially pronounced for elastomers with  $\text{TiO}_2$  fillers.

Figure 5 shows the Young's moduli and normalized Young's moduli as a function of strain after different post curing time spans for the pristine PDMS films RT625 and LR3040/30.

Normalised Young's moduli ( $Y_n(s)$ ) are calculated from  $Y_n(s) = \frac{Y(s)}{Y_0(s)}$ , where  $Y(s)$  is the Young's modulus for post cured elastomer films at a given strain, and  $Y_0$  is the corresponding Young's modulus for the non-post cured samples at the same strain. The effect of post

curing on the pristine elastomers is illustrated in Figure 5. Both investigated pristine elastomers show identical behavior with increased Young's moduli during increased post curing periods. The pristine elastomers both exhibit significant strain softening up to approximately 70% strain, following which strain hardening effects set in. This characteristic property of silicone elastomers leads to a local minimum in the Young's modulus as a function of strain. Strain hardening is particularly favorable in the context of avoiding the electromechanical instability (EMI) phenomenon which occurs when local Maxwell pressure exceeds the compressive stress of the elastomer<sup>[43–45]</sup>. The normalized Young's modulus plots (Figure 5b) show that LR3040/30 benefits on this occasion from post curing, since the curves become more strain hardening. The effect is less pronounced for RT625.

Young's moduli and normalized Young's moduli as functions of strain for RT625 and LR3040/30 with 35 phr  $\text{TiO}_2$  are shown in Figure 6.

The two different  $\text{TiO}_2$ -filled elastomers show very different responses in the Young's modulus as a function of strain. This is expected since the commercial formulations most likely consist of different types of silica fillers. The Young's modulus gives a clear indication of various interactions taking place at various strains, indicating the complex behavior of the composites with three types of overall interactions, namely, filler–filler, filler–polymer, and polymer–polymer interactions, where the introduction of the  $\text{TiO}_2$  fillers introduces additional two types of filler–filler interactions ( $\text{TiO}_2$ – $\text{TiO}_2$  and  $\text{TiO}_2$ –silica) as well as another filler–polymer interaction.

Filled LR3040/30 shows significantly more strain hardening and softening behaviors than filled RT625,

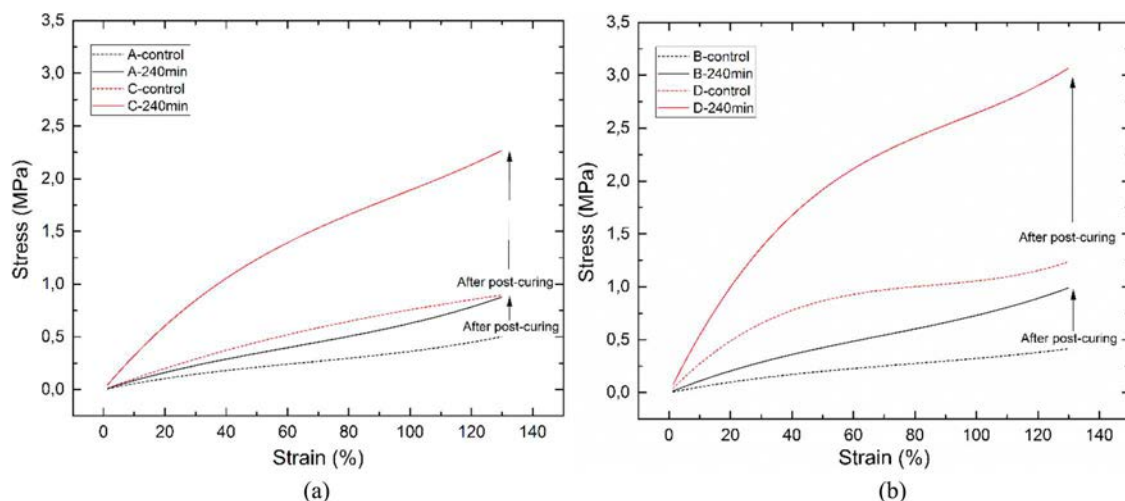


**Figure 4.** Stress–strain curves for left: Pristine RT625 (A) and RT625 with 35 phr  $\text{TiO}_2$ (C) and right: Pristine LR3040/30 (B) and LR3040/30 with 35 phr  $\text{TiO}_2$ (D).



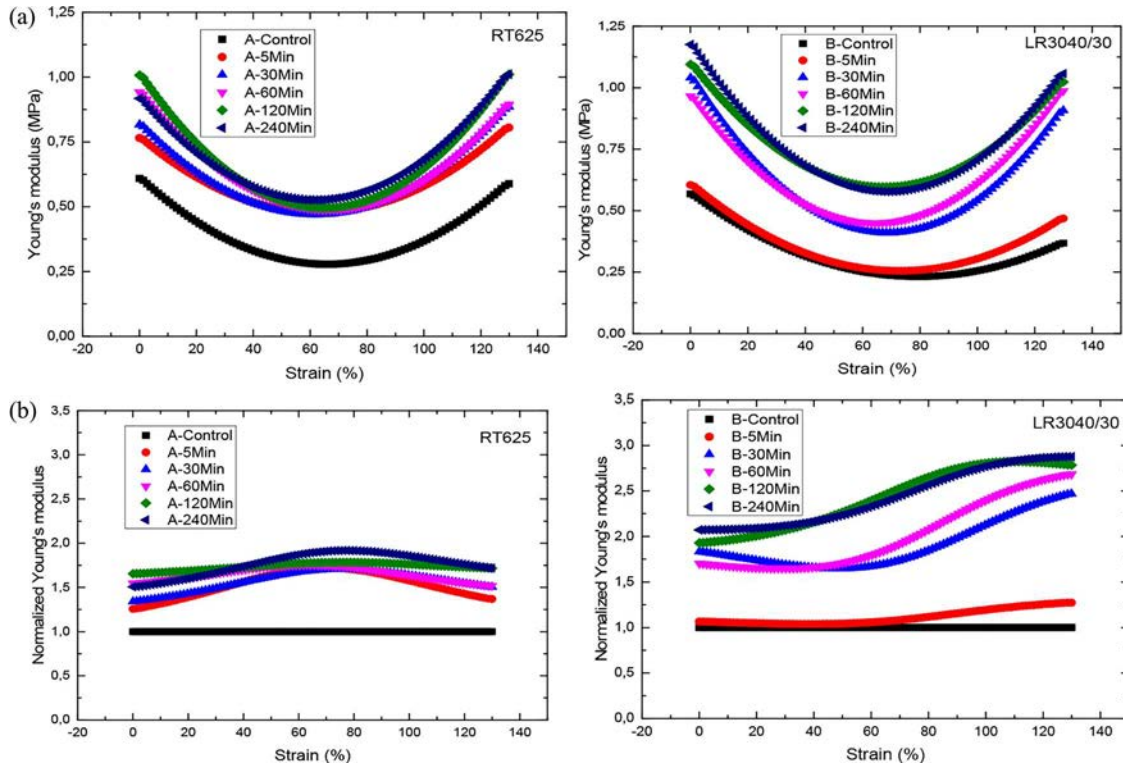


**Figure 5.** Young's modulus (a) and normalized Young's modulus (b) as a function of strain at different post curing periods for the pristine PDMS films (A = RT625 and B = LR3040/30).

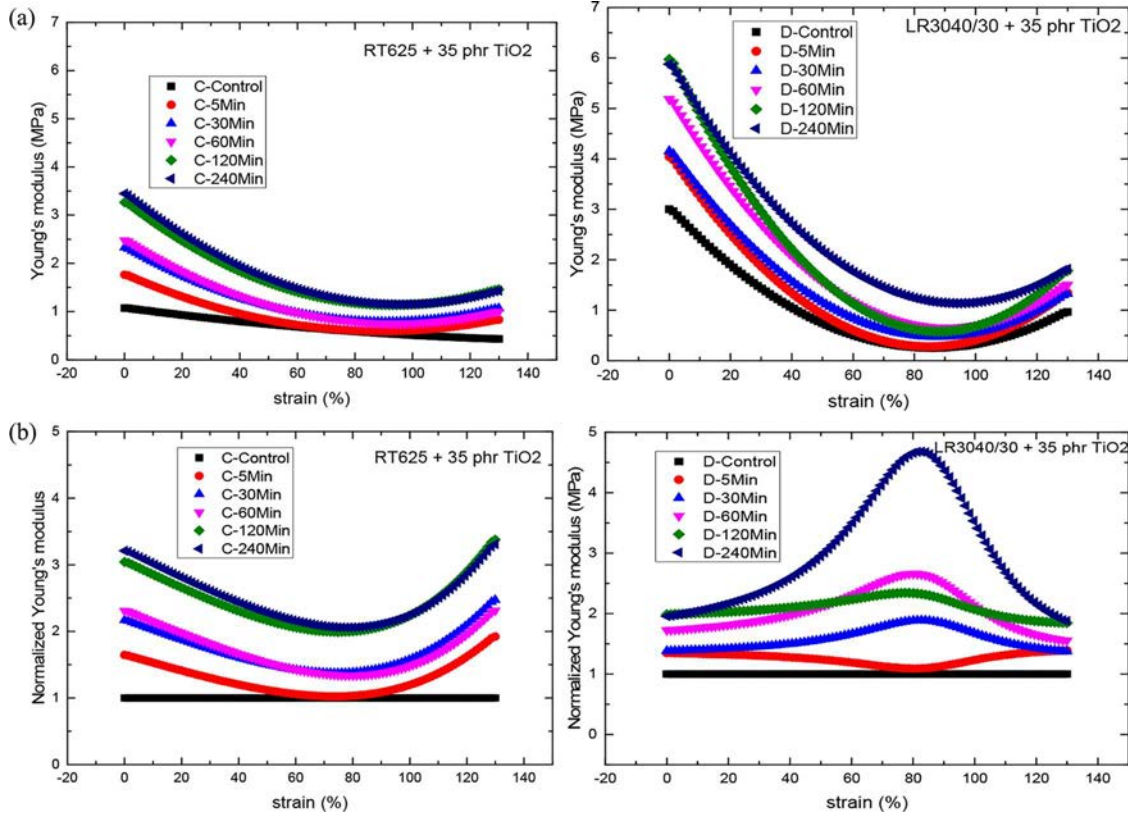
while the normalized Young's moduli plots as functions of strain (Figure 6b) also illustrate the different behaviors between the two elastomers. After post curing, the filled RT625 exhibits more strain-dependent effects than the nonpost cured control sample. LR3040/30, on the other hand, experiences very different effects. After post curing for longer than 5 min, the curves change shapes from concave to convex, with a peak maximum at approximately 85% strain. This phenomenon is only seen for the filled LR3040/30 elastomer and can be attributed to the high filler content within the elastomer. Up to a certain strain, the elastomer exhibits stress hardening behavior, where after stress softening sets in due to the high filler content, which in turn induces significant Mullins effects such as the rupture of filler clusters and the separation of weak polymer chains from the fillers<sup>[46]</sup>. The strain hardening that is experienced after post curing up to approximately 80% strain is, as mentioned previously, beneficial in the context of avoiding EMI. Post curing therefore improves this failure mode of filled DEs.

Figure 7 shows the storage modulus and loss ( $\tan \delta$ ) as a function of temperature at a constant strain and frequency.

It can be seen that all samples experience the same behavior, to a greater or lesser extent. After post curing, all materials have become significantly stiffer,

as illustrated by the increase in storage modulus. Before post curing, all samples experience a temperature-independent storage modulus, whereas thereafter the storage modulus drops as a function of temperature. Since the modulus drop is more pronounced for samples with high filler content, it may be ascribed to polymer–filler interactions such as the relaxation of polymer chains surrounding the fillers. Thus, for these samples, polymer–filler interactions are more pronounced than entropic elasticity, which would have led to storage modulus increases in line with increasing temperatures<sup>[47]</sup>. The losses are seen to decrease when the temperature increases, meaning that the samples become less dissipative at increasing temperatures. In the supporting information, time and frequency sweeps for different post cure time spans can be found for all samples. These results confirm that samples become stiffer after post curing and that no “actual” post curing (further cross-linking) takes place during the process, since the loss factor does not decrease thereafter.

Since post curing changes the Young's moduli of elastomers, dielectric breakdown strength may also be affected, as the breakdown strength of DE films has been found previously to scale linearly—or even exponentially—with the Young's modulus<sup>[14,37]</sup>. Table 2 shows dielectric breakdown strength and



**Figure 6.** Young's modulus (a) and a normalized Young's modulus (b) as a function of strain at different post curing periods for the filled PDMS films (C = RT625 + 35 phr TiO<sub>2</sub> and D = LR3040/30 + 35 phr TiO<sub>2</sub>).

Young's moduli at 5% strain at different post curing times. Dielectric breakdown strength as a function of Young's moduli at 5% strain is furthermore shown in Figure 8.

As expected, the breakdown strengths of elastomer samples increase as the Young's moduli increase. For both types of pristine elastomers, a maximum increase of 16–17% is obtained following post curing, which means that post curing effectively increases the dielectric breakdown strength of commercial DE films. Furthermore, the results show that the breakdown strength of heavily filled PDMS elastomers increases to a greater extent than for the pristine elastomers. The filled elastomers both experience an increase in breakdown strength of 33–34%, which is almost two-fold higher than for the pristine elastomers. This means that heavily filled elastomers benefit to a very great extent from post curing.

An analysis was performed to investigate the effect of post curing elastomer films on dielectric breakdown strength distribution. The Weibull distribution is one of the most commonly used methods in lifetime analysis and can provide insights into the electrical reliability of an elastomer. The breakdown data points ( $E_B$ ) are therefore fitted to the Weibull cumulative distribution

function,  $F(E_B)$ :

$$F(E_B) = 1 - \exp\left(-\frac{E_B}{\eta}\right)^\beta \quad (1)$$

which can be linearized to give:

$$\ln[-\ln(1 - F(E_B))] = \beta \cdot \ln(E_B) - \beta \cdot \ln(\eta). \quad (2)$$

The Weibull shape parameter,  $\beta$ , is equal to the slope of the regressed line. Different  $\beta$  values lead to noticeable effects on lifetime distribution, and  $\beta$  is also required to be as large as possible, such that the measured breakdown strengths all fall within a narrow range of voltages. This is furthermore an indication of homogeneity on the microscale. The Weibull scale parameter,  $\eta$ , which is determined from the distribution at which 63% of the films have broken down electrically, should be as high as possible and locate distribution along the scale. Table 3 shows the Weibull distribution results with  $\beta$ ,  $\eta$  and linear regression ( $r^2$ ) in a probability plot for control samples, and 240 min of post cured films.

The results show that post curing significantly increases the reliability of the tested elastomer films as the scale and the shape parameters increase. This

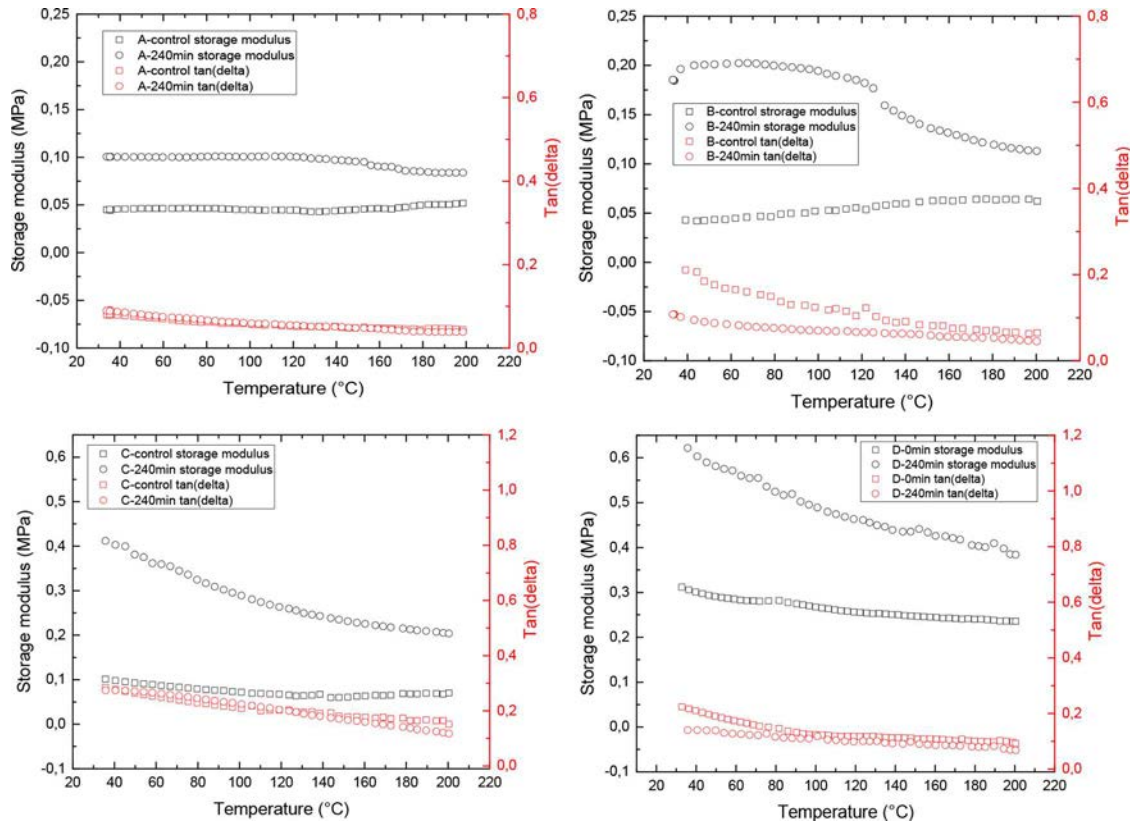
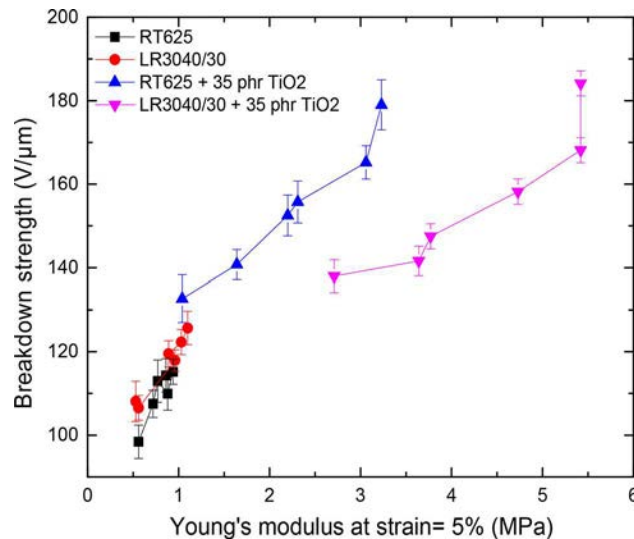


**Figure 7.** Storage modulus and loss ( $\tan \delta$ ) as a function of temperature before and after 240 min of post curing for (A = RT625, B = LR3040/30, C = RT625 + 35 phr TiO<sub>2</sub>, and D = LR3040/30 + 35 phr TiO<sub>2</sub>).

improvement is, among other things, attributed to the increase in the Young's modulus of the PDMS films upon post curing<sup>[37]</sup>. Post curing also extensively removes the volatiles that contribute to modulus inhomogeneities and defects which are introduced during film preparation<sup>[20]</sup>. Furthermore, since  $r^2$ , the linear regression goodness of fit values become closer to 1, and the breakdown data

thus become better fitted to the Weibull distribution after post curing. This again indicates that elastomers become more homogenous after post curing, since small-molecule inhomogeneities have been removed.

Figures 9 and 10 show the cumulative probability of failure, from which shape and scale parameters as well as  $r^2$  have been determined.

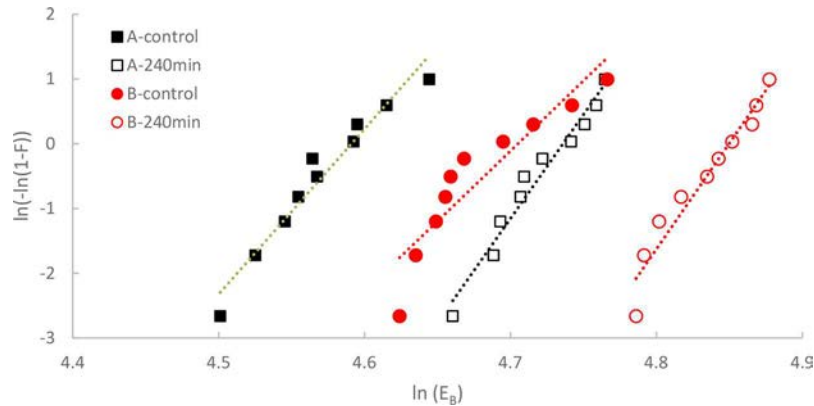
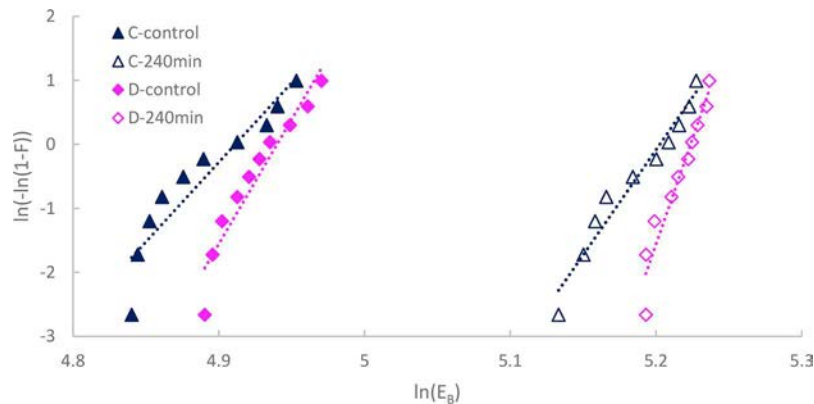


**Figure 8.** Breakdown strength as a function of the Young's modulus for the PDMS films. The Young's moduli for all tested samples are presented according to elevated post curing periods at 0-control, 5, 30, 60, 120, and 240 mins.

**Table 3.** Weibull parameters and  $r^2$  for the control and 240-min post cured films.

| Parameter                              | Scale ( $\eta$ ) (V/ $\mu\text{m}$ ) |                         | Shape ( $\beta$ ) |                         | $r^2$            |                         |
|--|--------------------------------------|-------------------------|-------------------|-------------------------|------------------|-------------------------|
|  | Before post cure                     | After post cure 240 min | Before post cure  | After post cure 240 min | Before post cure | After post cure 240 min |
| A (RT625)                              | 99                                   | 114                     | 27                | 33                      | 0.95             | 0.97                    |
| B (LR3040/30)                          | 110                                  | 127                     | 26                | 34                      | 0.85             | 0.94                    |
| C (RT625 + 35 phr $\text{TiO}_2$ )     | 135                                  | 182                     | 28                | 34                      | 0.88             | 0.96                    |
| D (LR3040/30 + 35 phr $\text{TiO}_2$ ) | 140                                  | 186                     | 42                | 71                      | 0.92             | 0.93                    |

phr, parts per hundred rubber.

**Figure 9.** Cumulative probability of pristine PDMS film failure before and after post curing (A = RT625 and B = LR3040/30).**Figure 10.** Cumulative probability of filled PDMS film failure before and after post curing (A = RT625 + 35 phr  $\text{TiO}_2$  and B = LR3040/30 + 35 phr  $\text{TiO}_2$ ).

It is clear from Figure 9 that sample B, before post curing, experiences breakdown behavior, with two clearly separated distributions signifying two breakdown processes. The first part of the data points is most likely due to small defects and filler agglomeration in the highly filled LR3040/30, whereas the second part of the data point distribution represents “true” breakdown processes. This behavior is significantly smaller after post curing, thereby indicating that post curing eliminates some of the causes of early breakdown phenomena, which can also be seen from the shape and scale parameters as well as the  $r^2$  values. The same behavior can be seen for the  $\text{TiO}_2$ -filled samples in

Figure 10, where both elastomers experience two breakdown distributions before post curing and where the behavior is significantly reduced thereafter.

## Conclusion

Four samples with different compositions were prepared, namely, a commercial RTV elastomer, RT625, a commercial LSR elastomer, LR3040/30, and the two mentioned elastomers with additional 35 phr added  $\text{TiO}_2$ . Important properties in relation to dielectric elastomers were measured before and after post cure treatment at 200°C for up to 240 min. This included



the effect of post curing on thermal properties, elastic/mechanical properties, and dielectric breakdown strength. This study shows that even commercial silicone elastomers require post curing for mechanical and electrical stability. This is an overlooked feature of silicone elastomers utilized in dielectric elastomers. The two commercial elastomers (RTV and LSR) both show improved strength over the post curing period. This phenomenon can be ascribed to the evaporation of volatiles and other residues from the PDMS films at high temperatures. In other words, the elastomer will not provide constant actuation over time, if it is not ensured that all volatiles have been removed beforehand. The removal of volatiles is furthermore favorable, as it increases electrical breakdown strength and thus enhances the reliability of the elastomer.

## Funding

The authors gratefully acknowledge financial support offered by the Ministry of Education of Malaysia and Universiti Malaysia Pahang. The Danish Council for Independent Research and Innovationsfonden Denmark are acknowledged for additional funding.

## References

- [1] Mark, J.E. *Silicon-Based Polymer Science: A Comprehensive Resource*, American Chemical Society, Oxford University Press: United Kingdom, 1990.
- [2] Brochu, P.; Pei, Q. Advances in dielectric elastomers for actuators and artificial muscles. *Macromol. Rapid Commun.* **2010**, *31*, 10–36.
- [3] Dünki, S.J.; Ko, Y.S.; Nüesch, F.A.; Opris, D.M. Self-Repairable, high permittivity dielectric elastomers with large actuation strains at low electric fields. *Adv. Funct. Mater.* **2015**, *25*, 2467–2475.
- [4] Madsen, F.B.; Yu, L.; Daugaard, A.E.; Hvilsted, S.; Skov, A.L. Self-Repairable, high permittivity dielectric elastomers with large actuation strains at low electric fields. *Polymer* **2014**, *55*, 6212–6219.
- [5] Kussmaul, B.; Risse, S.; Kofod, G.; Waché, R.; Wegener, M.; McCarthy, D.N.; Krüger, H.; Gerhard, R. Enhancement of dielectric permittivity and electromechanical response in silicone elastomers: molecular grafting of organic dipoles to the macromolecular network. *Adv. Funct. Mater.* **2011**, *21*, 4589–4594.
- [6] Madsen, F.B.; Javakhishvili, I.; Jensen, R.E.; Daugaard, A.E.; Hvilsted, S.; Skov, A.L. Synthesis of telechelic vinyl/allyl functional siloxane copolymers with structural control. *Polym. Chem.* **2014**, *5*, 7054–7061.
- [7] Yu, L.; Madsen, F.B.; Hvilsted, S.; Skov, A.L. Dielectric elastomers, with very high dielectric permittivity, based on silicone and ionic interpenetrating networks. *RSC Adv.* **2015**, *5*, 49739–49747.
- [8] Tugui, C.; Stiubianu, G.T.; Iacob, M.; Ursu, C.; Bele, A.; Vlad, S.; Cazacu, M.J. Bimodal silicone interpenetrating networks sequentially built as electroactive dielectric elastomers. *Mater. Chem. C* **2015**, *3*, 8963–8969.
- [9] Ha, S.M.; Yuan, W.; Pei, Q.; Pelrine, R.; Stanford, S. Interpenetrating networks of elastomers exhibiting 300% electrically-induced strain. *Smart Mater. Struct.* **2007**, *16*, S280–S287.
- [10] Ha, S.M.; Wissler, M.; Pelrine, R.; Stanford, S.; Kovacs, G.; Pei, Q. Characterization of electroelastomers based on interpenetrating polymer networks. *Proc. SPIE* **2007**, *6524*, 652408–652408–10.
- [11] Brochu, P.; Stoyanov, H.; Niu, X.; Pei, Q. All-silicone prestrain-locked interpenetrating polymer network elastomers: free-standing silicone artificial muscles with improved performance and robustness. *Smart Mater. Struct.* **2013**, *22*, 055022.
- [12] Carpi, F.; Gallone, G.; Galantini, F.; De Rossi, D. Silicone-Poly(hexylthiophene) blends as elastomers with enhanced electromechanical transduction properties. *Adv. Funct. Mater.* **2008**, *18*, 235–241.
- [13] Madsen, F.B.; Yu, L.; Mazurek, P.S.; Skov, A.L. A simple method for reducing inevitable dielectric loss in high-permittivity dielectric elastomers. *Smart Mater. Struct.* **2016**, *25*, 7. Article number 075018.
- [14] Vudayagiri, S.; Zakaria, S.; Yu, L.; Hassouneh, S.S.; Benslimane, M.; Skov, A.L. High breakdown-strength composites from liquid silicone rubbers. *Smart Mater. Struct.* **2014**, *23*, 105017.
- [15] Wang, G.L.; Zhang, Y.Y.; Duan, L.; Ding, K.H.; Wang, Z. F.; Zhang, M.J. Property reinforcement of silicone dielectric elastomers filled with self-prepared calcium copper titanate particles. *Appl. Polym. Sci.* **2015**, *132*, 42613.
- [16] Vudayagiri, S.; Junker, M.D.; Skov, A.L. Factors affecting surface and release properties of thin PDMS films. *Polym. J.* **2013**, *45*, 871–878.
- [17] Carpi, F.; De Rossi, D.; Kornbluh, R.; Pelrine, R.; Sommer-Larsen, P. *Dielectric Elastomers as Electromechanical Transducers: Fundamentals, Materials, Devices, Models and Applications of an Emerging Electroactive Polymer Technology*, Elsevier Ltd: Oxford, UK, 2008.
- [18] Rosset, S.; Maffli, L.; Houis, S.; Shea, H.R. An instrument to obtain the correct biaxial hyperelastic parameters of silicones for accurate DEA modeling. *Proc. SPIE* **2014**, *9056*, 90560M–1–90560M–12.
- [19] Noll, W. *Chemistry and Technology of Silicones*, Academic: New York, 1968.
- [20] Brook, M.A.; Saier, H.U.; Schnabel, J.; Town, K.; Maloney, M. Pretreatment of liquid silicone rubbers to remove volatile siloxanes. *Ind. Eng. Chem. Res.* **2007**, *46*, 8796–8805.
- [21] Villahermosa, R.M.; Ostrowski, A.D. Chemical analysis of silicone outgassing. *Proc. SPIE* **2008**, *7069*, 706906–1–706906–10.
- [22] Malinconico, M.; Immirzi, B.; Massenti, S.; La Mantia, F. P.; Mormile, P.; Petti, L.J. Blends of polyvinylalcohol and functionalised polycaprolactone. A study on the melt extrusion and post-cure of films suitable for protected cultivation. *Mater. Sci.* **2002**, *37*, 4973–4978.
- [23] Jansen, J.A.J.; Haas, W.E.; Neutkens, H.G.M.; Leenen, A.J.H. Blends of polyvinylalcohol and functionalised polycaprolactone. A study on the melt extrusion and post-cure of films suitable for protected cultivation. *Thermochim. Acta* **1988**, *134*, 307–312.



- [24] Dyakonov, T.; Chen, Y.; Holland, K.; Drbohlav, J.; Bums, D.; Vander Velde, D.; Seih, L.; Soloski, E.J.; Kuhn, J.; Mann, P.J.; Stevenson, W.T.K. Thermal analysis of some aromatic amine cured model epoxy resin systems-I: Materials synthesis and characterization, cure and post-cure. *Polym. Degrad. Stab.* **1996**, *3910*, 217–242.
- [25] Wu, C.S. J. Influence of post-curing and temperature effects on bulk density, glass transition and stress-strain behaviour of imidazole-cured epoxy network. *Mater. Sci.* **1992**, *27*, 2952–2959.
- [26] Ko, T.-H.; Kuo, W.-S.; Lu, Y.-R. The influence of post-cure on properties of carbon/phenolic resin cured composites and their final carbon/carbon composites. *Polym. Compos.* **2000**, *21*, 96–103.
- [27] Rothka, J.; Studd, R.; Tate, K.; Timpe, D. *Outgassing of Silicone Elastomers*, ArlonSilicone Technology Division, ISC: Bear, DE, 2000.
- [28] Madsen, F.B.; Daugaard, A.E.; Hvilsted, S.; Benslimane, M.Y.; Skov, A.L. Dipolar cross-linkers for PDMS networks with enhanced dielectric permittivity and low dielectric loss. *Smart Mater. Struct.* **2013**, *22*, 104002.
- [29] Bele, A.; Cazacu, M.; Racles, C.; Stiubianu, G.; Ovezza, D.; Ignat, M. Tuning the electromechanical properties of silicones by crosslinking agent. *Adv. Eng. Mater.* **2015**, *17*, 1302–1312.
- [30] Opris, D.M.; Molberg, M.; Walder, C.; Ko, Y.S.; Fischer, B.; Nüesch, F.A. New silicone composites for dielectric elastomer actuator applications in competition with acrylic foil. *Adv. Funct. Mater.* **2011**, *21*, 3531–3539.
- [31] Gallone, G.; Galantini, F.; Carpi, F. Perspectives for new dielectric elastomers with improved electromechanical actuation performance: Composites versus blends. *Polym. Int.* **2010**, *59*, 400–406.
- [32] Ouyang, G.; Wang, K.; Chen, X.Y. TiO<sub>2</sub> nanoparticles modified polydimethylsiloxane with fast response time and increased dielectric constant. *J. Micromech. Microeng.* **2012**, *22*, 074002.
- [33] Stoyanov, H.; Brochu, P.; Niu, X.; Della Gaspera, E.; Pei, Q. Dielectric elastomer transducers with enhanced force output and work density. *Appl. Phys. Lett.* **2012**, *100*, 262902.
- [34] Romasanta, L.J.; Leret, P.; Casaban, L.; Hernández, M.; de la Rubia, M.A.; Fernández, J.F.; Kenny, J.M.; Lopez-Manchado, M.A.; Verdejo, R.J. Towards materials with enhanced electro-mechanical response: CaCu<sub>3</sub>Ti<sub>4</sub>O<sub>12</sub>-polydimethylsiloxane composites. *Mater. Chem.* **2012**, *22*, 24705–24712.
- [35] Zhao, H.; Wang, D.-R.; Zha, J.-W.; Zhao, J.; Dang, Z.-M. Increased electroaction through a molecular flexibility tuning process in TiO<sub>2</sub>-polydimethylsilicone nanocomposites. *J. Mater. Chem. A* **2013**, *1*, 3140–3145.
- [36] Zakaria, S.; Yu, L.; Kofod, G.; Skov, A.L. The influence of static pre-stretching on the mechanical ageing of filled silicone rubbers for dielectric elastomer applications. *Mater. Today Commun.* **2015**, *4*, 204–213.
- [37] Kollosche, M.; Stoyanov, H.; Ragusch, H.; Risse, S.; Becker, A.; Kofod, G. Electrical breakdown in soft elastomers: stiffness dependence in un-pre-stretched elastomers, 2010 10th IEEE International Conference on Solid Dielectrics, Potsdam, 1–4, 2010.
- [38] Vudayagiri, S.; Yu, L.; Hassounieh, S.S.; Skov, A.L. Hot embossing of microstructures on addition curing polydimethylsiloxane films. *J. Elastomers Plast.* **2013**, *46*, 623–643.
- [39] Vudayagiri, S.; Skov, A.L. Methods to ease the release of thin polydimethylsiloxane films from difficult substrates. *Polym. Adv. Technol.* **2014**, *25*, 249–257.
- [40] Vudayagiri, S.; Yu, L.; Hassounieh, S.S.; Hansen, U.; Skov, A.L. Bilaterally microstructured thin polydimethylsiloxane film production. *Polym. Plast. Technol. Eng.* **2015**, *54*, 425–432.
- [41] Skov, A.L.; Vudayagiri, S.; Benslimane, M. Novel silicone elastomer formulations for DEAPs. *Proc. SPIE* **2013**, *8687*, 86871I–86871I–8.
- [42] Benslimane, M.; Kiil, H.-E.; Tryson, M.J. Electromechanical properties of novel large strain polypower film and laminate components for DEAP actuator and sensor applications. *Proc. SPIE* **2010**, *7642*, 764231–764231–11.
- [43] Zhao, X.; Suo, Z. Theory of dielectric elastomers capable of giant deformation of actuation. *Phys. Rev. Lett.* **2010**, *104*, 1–4.
- [44] Gatti, D.; Haus, H.; Matysek, M.; Frohnapfel, B.; Tropea, C.; Schlaak, H.F. The dielectric breakdown limit of silicone dielectric elastomer actuators. *Appl. Phys. Lett.* **2014**, *104*, 052905.
- [45] Stark, K.H.; Garton, C.G. Electric strength of irradiated polythene. *Nature* **1955**, *176*, 1225–1226.
- [46] Dorfmann, A.; Ogden, R.W. A constitutive model for the Mullins effect with permanent set in particle-reinforced rubber. *Int. J. Solids Struct.* **2004**, *41*, 1855–1878.
- [47] Stricher, A.M.; Rinaldi, R.G.; Barrès, C.; Ganachaud, F.; Chazeau, L. How I met your elastomers: from network topology to mechanical behaviours of conventional silicone materials. *RSC Adv.* **2015**, *5*, 53713–53725.